

Rare Earth-Transition Metal Indides with $\text{Lu}_5\text{Ni}_2\text{In}_4$ -type Structure

Roman Zaremba, Wilfried Hermes, Matthias Eul, and Rainer Pöttgen

Institut für Anorganische und Analytische Chemie, Universität Münster, Corrensstrasse 30, D-48149 Münster, Germany

Reprint requests to R. Pöttgen.
E-mail: pottgen@uni-muenster.de

Z. Naturforsch. **2008**, *63b*, 1447–1449; received September 4, 2008

New intermetallic compounds $\text{RE}_5\text{T}_2\text{In}_4$ ($\text{RE} = \text{Sc}, \text{Y}, \text{La-Nd}, \text{Sm}, \text{Gd-Tm}, \text{Lu}; \text{T} = \text{Rh}, \text{Ir}$) were synthesized by arc-melting of the elements or by induction melting of the elements in tantalum crucibles under flowing argon. The samples were characterized by X-ray powder diffraction. They crystallize with the orthorhombic $\text{Lu}_5\text{Ni}_2\text{In}_4$ -type structure, space group $Pbam$, $Z = 2$, a 2:1 intergrowth variant of CsCl and AlB_2 related slabs of compositions InRE_8 (distorted cubes) and RhRE_6 (distorted trigonal prisms). Susceptibility measurements of $\text{Ce}_5\text{Ir}_2\text{In}_4$ have revealed modified Curie-Weiss behavior above 70 K with an experimental magnetic moment of $2.45(1) \mu_{\text{B}}/\text{Ce}$ atom. The cerium magnetic moments order ferri- or ferromagnetically at $T_{\text{C}} = 7.1(2)$ K.

Key words: Intermetallics, Indium, Crystal Chemistry

Introduction

The ternary systems RE-T-In ($\text{RE} =$ rare earth metal, $\text{T} =$ late transition metal) contain a variety of compounds with comparatively large unit cells and complex crystal structures [1]. A deeper analysis of the near-neighbor coordination, however, often shows that these complex structures can be considered as simple intergrowth variants of slightly distorted slabs of well known binary structure types, *viz.* AlB_2 , Cu_3Au , CsCl , Zr_4Al_3 , or CaCu_5 . For the indide structures several structure types are composed of CsCl (REIn) and AlB_2 (RET_2) slabs, and they can be described by the general formula $\text{RE}_{m+n}\text{T}_2\text{In}_m$, where m and n are the numbers of CsCl and AlB_2 related slabs.

The structure type $\text{Lu}_5\text{Ni}_2\text{In}_4$ [2] is the $m = 8$ and $n = 2$ member of the latter series. Besides the series $\text{RE}_5\text{Ni}_2\text{In}_4$ [2, 3], also representatives with $\text{T} = \text{Pd}$ [4] and Pt [5, 6] have been synthesized. Interestingly, this

structure type also exists for $\text{Zr}_5\text{Rh}_2\text{In}_4$ and $\text{Hf}_5\text{Rh}_2\text{In}_4$ [7] with a much higher valence electron concentration. $\text{Zr}_5\text{Ir}_2\text{In}_4$ [8] forms a new superstructure variant of the $\text{Lu}_5\text{Ni}_2\text{In}_4$ type.

In continuation of our systematic phase analytical investigations of the RE-T-In systems we have now synthesized the $\text{RE}_5\text{T}_2\text{In}_4$ indides with rhodium and iridium as the transition metal component.

Experimental Section

Synthesis

Starting materials for the synthesis of the $\text{RE}_5\text{Rh}_2\text{In}_4$ and $\text{RE}_5\text{Ir}_2\text{In}_4$ samples were ingots of the rare earth metals (Johnson Matthey or smart elements), rhodium and iridium powder (Degussa-Hüls, *ca.* 200 mesh), and indium tear drops (Johnson Matthey), all with stated purities better than 99.9%. Pieces of the rare earth ingots were first arc-melted [9] to small buttons under an argon atmosphere. The argon was purified before with molecular sieves, silica gel, and titanium sponge (900 K). Subsequently the rare earth buttons, cold-pressed pellets of the rhodium (iridium) powder and pieces of the indium tear drops (5:2:4 atomic ratio) were arc-melted. The product buttons were remelted three times to ensure homogeneity. The weight loss after the different melting procedures was always smaller than 0.5%. Alternatively, the $\text{RE}_5\text{Rh}_2\text{In}_4$ samples could also be prepared by induction melting of the elements in small tantalum crucibles (\varnothing 8 mm) in a water-cooled sample chamber of an induction furnace (Hüttinger Elektronik, Freiburg, and type TIG 1.5/300) under flowing argon [10], similar to the $\text{RE}_5\text{Pt}_2\text{In}_4$ compounds [6]. The polycrystalline $\text{RE}_5\text{Rh}_2\text{In}_4$ and $\text{RE}_5\text{Ir}_2\text{In}_4$ samples are stable in air over weeks.

X-Ray powder diffraction

The powdered polycrystalline samples were studied through Guinier patterns (imaging plate detector, Fujifilm BAS-1800 readout system) using $\text{CuK}\alpha_1$ radiation and α -quartz ($a = 491.30$ and $c = 540.46$ pm) as an internal standard. The orthorhombic lattice parameters (Table 1) were obtained from the powder data by least-squares calculations. The correct indexing was ensured through intensity calculations [11].

Magnetic measurements

24.064 mg of the $\text{Ce}_5\text{Ir}_2\text{In}_4$ sample were packed in kapton foil and attached to the sample holder rod of a VSM for measuring the magnetic properties in a Quantum Design

Table 1. Lattice parameters (Guinier powder data) of the ternary indium compounds with $\text{Lu}_5\text{Ni}_2\text{In}_4$ -type structure.

Compound	<i>a</i> (pm)	<i>b</i> (pm)	<i>c</i> (pm)	<i>V</i> (nm ³)
<i>RE</i>₅<i>Rh</i>₂<i>In</i>₄:				
$\text{Y}_5\text{Rh}_2\text{In}_4$	1810.1(9)	799.0(3)	362.5(2)	0.5243
$\text{Pr}_5\text{Rh}_2\text{In}_4$	1840.1(6)	814.0(4)	376.2(1)	0.5635
$\text{Nd}_5\text{Rh}_2\text{In}_4$	1835.9(9)	812.3(4)	374.5(2)	0.5584
$\text{Sm}_5\text{Rh}_2\text{In}_4$	1825(2)	805(1)	370.2(3)	0.5438
$\text{Gd}_5\text{Rh}_2\text{In}_4$	1819.0(9)	800.7(4)	366.0(3)	0.5330
$\text{Tb}_5\text{Rh}_2\text{In}_4$	1817(2)	799.1(7)	365.1(4)	0.5302
$\text{Dy}_5\text{Rh}_2\text{In}_4$	1806.1(7)	795.1(4)	360.6(2)	0.5179
$\text{Ho}_5\text{Rh}_2\text{In}_4$	1802.1(8)	793.7(3)	358.5(2)	0.5128
$\text{Er}_5\text{Rh}_2\text{In}_4$	1797.6(7)	791.3(3)	356.0(2)	0.5064
$\text{Tm}_5\text{Rh}_2\text{In}_4$	1795.4(5)	789.8(2)	354.5(1)	0.5027
$\text{Lu}_5\text{Rh}_2\text{In}_4$	1786.1(9)	786.1(9)	350.6(2)	0.4927
<i>RE</i>₅<i>Ir</i>₂<i>In</i>₄:				
$\text{Sc}_5\text{Ir}_2\text{In}_4$	1765(2)	772.9(5)	330.2(3)	0.4504
$\text{Y}_5\text{Ir}_2\text{In}_4$	1810(2)	800.6(6)	361.3(3)	0.5236
$\text{La}_5\text{Ir}_2\text{In}_4$	1858.9(9)	831.1(7)	383.9(2)	0.5931
$\text{Ce}_5\text{Ir}_2\text{In}_4$	1848.8(6)	815.2(4)	378.1(1)	0.5699
$\text{Pr}_5\text{Ir}_2\text{In}_4$	1840.0(6)	817.2(2)	377.9(2)	0.5683
$\text{Nd}_5\text{Ir}_2\text{In}_4$	1836(1)	814.1(5)	375.5(2)	0.5611
$\text{Gd}_5\text{Ir}_2\text{In}_4$	1816(1)	803.1(5)	367.0(3)	0.5351
$\text{Tb}_5\text{Ir}_2\text{In}_4$	1818(2)	801(1)	362.9(3)	0.5285
$\text{Dy}_5\text{Ir}_2\text{In}_4$	1802(1)	797.9(5)	361.0(2)	0.5189

Physical-Property-Measurement-System in the temperature range 2.1 – 305 K with magnetic flux densities up to 80 kOe.

Discussion

Synthesis conditions and crystal chemistry

Twenty new representatives of the $\text{RE}_5\text{Rh}_2\text{In}_4$ and $\text{RE}_5\text{Ir}_2\text{In}_4$ series with the $\text{Lu}_5\text{Ni}_2\text{In}_4$ -type structure have been synthesized and structurally characterized on the basis of X-ray powder diffraction. As is evident from Table 1, the cell volumes decrease with increasing ordering number of the rare earth elements, as expected from the lanthanoid contraction. Similar to the $\text{RE}_5\text{Pt}_2\text{In}_4$ series [6], the cell volumes of $\text{Y}_5\text{Rh}_2\text{In}_4$ and $\text{Y}_5\text{Ir}_2\text{In}_4$ also fit in between the terbium and dysprosium compounds. $\text{Sc}_5\text{Ir}_2\text{In}_4$ and the recently reported $\text{Sc}_5\text{Rh}_2\text{In}_4$ [3] have the by far smallest cell volumes in the two series.

So far it was not possible to obtain well shaped single crystals of the $\text{RE}_5\text{Rh}_2\text{In}_4$ and $\text{RE}_5\text{Ir}_2\text{In}_4$ indides. As already observed for $\text{Sc}_5\text{Ni}_2\text{In}_4$ and $\text{Sc}_5\text{Rh}_2\text{In}_4$ [3], we obtained only loose agglomerates of lath-shaped smaller crystals, or the samples were completely polycrystalline. Nevertheless, the Guinier powder data undoubtedly confirm the $\text{Lu}_5\text{Ni}_2\text{In}_4$ type for all samples.

The X-ray powder patterns of the $5\text{RE}:2\text{Rh}:4\text{In}$ samples with $\text{RE} = \text{La}$ and Ce , and the $5\text{RE}:2\text{Ir}:4\text{In}$

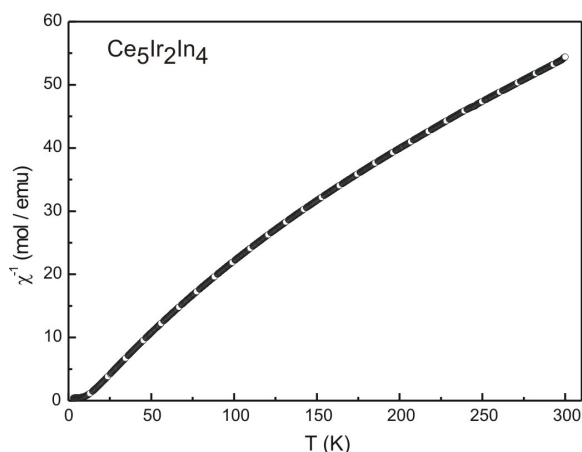


Fig. 1. Temperature dependence of the reciprocal magnetic susceptibility (χ^{-1} data) of $\text{Ce}_5\text{Ir}_2\text{In}_4$ measured at 10 kOe.

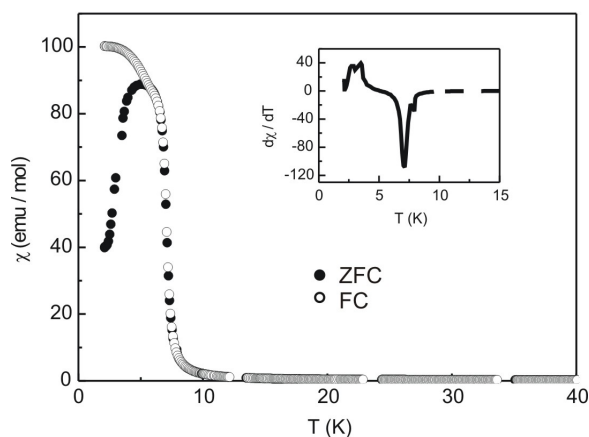


Fig. 2. Low-temperature susceptibility (zero field cooling and field cooling modus) of $\text{Ce}_5\text{Ir}_2\text{In}_4$ at 100 Oe (kink-point measurement). The inset shows the derivative $d\chi/dT$ of the zero field cooling curve with a sharp peak at the Curie temperature of $T_C = 7.1$ K.

samples with $\text{RE} = \text{Sm}$, Ho – Tm and Lu gave no hint for the formation of $\text{Lu}_5\text{Ni}_2\text{In}_4$ -type phases. The samples were multi-phase. More detailed studies of these systems are in progress.

Magnetic properties of Ce₅Ir₂In₄

The temperature dependence of the reciprocal magnetic susceptibility of $\text{Ce}_5\text{Ir}_2\text{In}_4$ is presented in Fig. 1. Above 70 K, $\chi^{-1} = f(T)$ was analyzed using the modified Curie-Weiss expression $\chi^{-1} = 1/(\chi_0 + C/(T - \theta_p))$ where θ_p is the asymptotic Curie temperature, C is the Curie constant, and χ_0 includes the temperature independent Van Vleck correction, the dia-

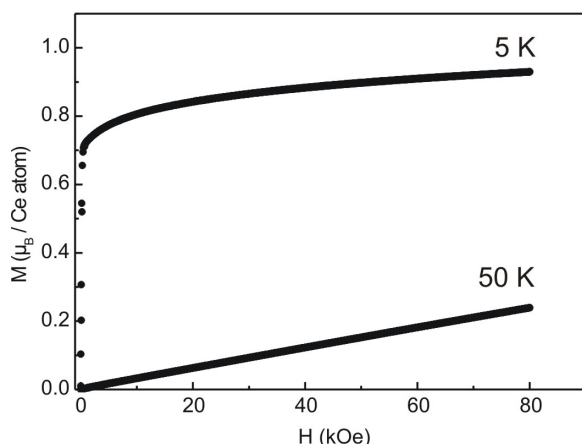


Fig. 3. Magnetization isotherms of $\text{Ce}_5\text{Ir}_2\text{In}_4$ measured at 5 and 50 K.

magnetic core correction and the paramagnetic contribution of the conduction electrons. The values of θ_p , χ_0 and $\mu_{\text{eff}} = (8C)^{1/2}$ have been refined by a least-squares method giving $\theta_p = 4.6(1)$ K, $\chi_0 = 5.7 \times 10^{-3}$ emu mol $^{-1}$ and $\mu_{\text{eff}} = 2.45(1)$ μ_B /Ce atom for $\text{Ce}_5\text{Ir}_2\text{In}_4$. The experimentally determined moment is close to the free ion value of 2.54 μ_B for Ce^{3+} .

At low temperature the susceptibility curve shows an anomaly below 11 K indicating ferri- or ferromagnetic ordering. The exact Curie temperature was de-

termined from a kink-point measurement (Fig. 2). We have therefore measured the susceptibility in a low external field of 100 Oe in zero field cooling and field cooling mode. The derivative $d\chi/dT$ of the field cooling measurement resulted in a Curie temperature of $T_C = 7.1(2)$ K. Similar magnetic behavior was observed for CeNiIn_2 [12].

The magnetization isotherms taken at 5 and 50 K are shown in Fig. 3. At 50 K we observe an almost linear increase of the magnetization with the applied field as expected for a paramagnetic material. In contrast, at 5 K the magnetization almost reaches saturation at an external field strength of 1 T, and the saturation magnetization (m) at 80 kOe amounts to $\mu_{\text{exp}(sm)} = 0.93(1)$ μ_B /Ce atom, significantly reduced from the theoretical value for Ce^{3+} at 2.14 μ_B /Ce atom. Saturation moments in the range of 1 μ_B /Ce atom are frequently observed for similar ternary intermetallics, e. g. for CeNiIn_2 [12], CeAuGe [13], CeRhSn_2 [14] or the silicides Ce_2TSi_3 [15]. These small values of the saturation are due to crystal field splitting effects on the $J = 5/2$ ground state of the Ce^{3+} ion. In view of the three crystallographically independent cerium sites, the magnetic structure is expected to be complex.

Acknowledgement

This work was supported by the Deutsche Forschungsgemeinschaft.

- [1] Ya. M. Kalychak, V. I. Zaremba, R. Pöttgen, M. Lukachuk, R.-D. Hoffmann, in *Handbook on the Physics and Chemistry of Rare Earths*, Vol. 34, (Eds.: K. A. Gschneidner, Jr., V. K. Pecharsky, J.-C. Bünzli), Elsevier, Amsterdam, **2005**, chapter 218, p. 1.
- [2] V. I. Zaremba, Ya. M. Kalychak, P. Yu. Zavalii, V. A. Bruskov, *Krystallografiya* **1991**, *36*, 1415.
- [3] M. Lukachuk, B. Heying, U. Ch. Rodewald, R. Pöttgen, *Heteroatom Chem.* **2005**, *16*, 364.
- [4] L. Sojka, M. Daszkiewicz, B. Belan, M. Manyako, V. Davydov, L. Akselrud, Ya. Kalychak, X. I. Sci. Conf. "Lviv Chemical Reading-2007", Coll. Abstr., Lviv **2007**, H51.
- [5] A. I. Tursina, Z. M. Kurenbaeva, D. V. Shepta, S. N. Nesterenko, H. Noël, *Acta Crystallogr. E* **2006**, *62*, i80.
- [6] R. Zaremba, U. Ch. Rodewald, R. Pöttgen, *Monatsh. Chem.* **2007**, *138*, 819.
- [7] M. Lukachuk, R. Pöttgen, *Z. Naturforsch.* **2002**, *57b*, 1353.
- [8] M. Lukachuk, R.-D. Hoffmann, R. Pöttgen, *Monatsh. Chem.* **2005**, *136*, 127.
- [9] R. Pöttgen, Th. Gulden, A. Simon, *GIT Labor-Fachzeitschrift* **1999**, *43*, 133.
- [10] D. Kußmann, R.-D. Hoffmann, R. Pöttgen, *Z. Anorg. Allg. Chem.* **1998**, *624*, 1727.
- [11] K. Yvon, W. Jeitschko, E. Parthé, *J. Appl. Crystallogr.* **1977**, *10*, 73.
- [12] V. I. Zaremba, Ya. M. Kalychak, Yu. B. Tyvanchuk, R.-D. Hoffmann, M. H. Möller, R. Pöttgen, *Z. Naturforsch.* **2002**, *57b*, 791.
- [13] R. Pöttgen, H. Borrmann, R. K. Kremer, *J. Magn. Magn. Mater.* **1996**, *152*, 196.
- [14] D. Niepmann, R. Pöttgen, B. Künnen, G. Kotzyba, C. Rosenhahn, B. D. Mosel, *Chem. Mater.* **1999**, *11*, 1597.
- [15] R. A. Gordon, C. J. Warren, M. G. Alexander, F. J. DiSalvo, R. Pöttgen, *J. Alloys Compd.* **1997**, *248*, 24.